UNCLASSIFIED MASTER COPY - FOR REPRODUCTION PURPOSES

AD-A206 156

EPORT DOCUMENTATION PAGE

1b. RESTRICTIVE MARKINGS

3 DISTRIBUTION / AVAILABILITY OF REPORT
Approved for public release; distribution unlimited.

2b. DECLASSIFICATION / DOWNGRADING SCHEDULE

4. PERFORMING ORGANIZATION REPORT NUMBER(S)

5. MONITORING ORGANIZATION REPORT NUMBER(S)
ARO 23525.27-EG

6a. NAME OF PERFORMING ORGANIZATION
Department of Mechanical Engineering

6b OFFICE SYMBOL (If applicable)

7a. NAME OF MONITORING ORGANIZATION
U. S. Army Research Office

6c. ADDRESS (City, State, and ZIP Code)
110 8th Street
Rensselaer Polytechnic Institute
Troy, NY 12180-3590

7b. ADDRESS (City, State, and ZIP Code)
P. O. Box 12211
Research Triangle Park, NC 27709-2211

8a. NAME OF FUNDING / SPONSORING ORGANIZATION
U. S. Army Research Office

8b. OFFICE SYMBOL (If applicable)

9. PROCUREMENT INSTRUMENT IDENTIFICATION NUMBER
DAAL03-86-K-0076

8c. ADDRESS (City, State, and ZIP Code)
P. O. Box 12211
Research Triangle Park, NC 27709-2211

10. SOURCE OF FUNDING NUMBERS

PROGRAM ELEMENT NO.	PROJECT NO.	TASK NO.	WORK UNIT ACCESSION NO

11. TITLE (Include Security Classification)
Steel Hardness Effects in Boundary Lubricated Sliding: An In-Situ SEM Study

12. PERSONAL AUTHOR(S)
W. Holzhauer and S.J. Calabrese

13a. TYPE OF REPORT	13b. TIME COVERED FROM ____ TO ____	14. DATE OF REPORT (Year, Month, Day)	15. PAGE COUNT

16. SUPPLEMENTARY NOTATION
The view, opinions and/or findings contained in this report are those of the author(s) and should not be construed as an official Department of the Army position, policy, or decision, unless so designated by other documentation.

17. COSATI CODES		
FIELD	GROUP	SUB-GROUP

18. SUBJECT TERMS (Continue on reverse if necessary and identify by block number)
SEM, Wear, Boundary Lubrication, Hardness

19 ABSTRACT (Continue on reverse if necessary and identify by block number)

A pin–on cylinder test apparatus was used to perform low speed, steel–on–steel sliding experiments in–situ in a scanning electron microscope (SEM). Through modifications to the SEM, these experiments could be run with a thin film of hydrocarbon oil applied to the sliding surface. Studies have been performed using AISI 4340 steel, both annealed and through hardened, for the pin and cylinder in combinations of soft (annealed)–versus–soft, hard–versus–soft and hard–versus–hard.

All three material combinations show a progressive smoothing in the wear track as the number of sliding passes increases, plus agglomeration of wear debris interspersed with oil around the contact. Both of these effects lead to failure of the contacts due to insufficient lubrication. The combinations involving annealed steel fail catastrophically by an apparent third body abrasive mechanism while the failure of the hard versus hard combination involves intermittent plowing, resulting in more localized damage.

20 DISTRIBUTION / AVAILABILITY OF ABSTRACT
☐ UNCLASSIFIED/UNLIMITED ☐ SAME AS RPT. ☐ DTIC USERS

21. ABSTRACT SECURITY CLASSIFICATION
Unclassified

22a. NAME OF RESPONSIBLE INDIVIDUAL

22b. TELEPHONE (Include Area Code) | 22c. OFFICE SYMBOL

DD FORM 1473, 84 MAR 83 APR edition may be used until exhausted. All other editions are obsolete.

SECURITY CLASSIFICATION OF THIS PAGE
UNCLASSIFIED

DTIC ELECTE S 2 1 MAR 1989

PREPRINT NO. 88-TC-2E-1
STLE PREPRINTS

Steel Hardness Effects in Boundary Lubricated Sliding: An In-Situ SEM Study©

W. Holzhauer* (STLE) and S. J. Calabrese (STLE)
Rensselaer Polytechnic Institute
Troy, New York 12180-3590

A pin-on-cylinder test apparatus was used to perform low speed, steel-on-steel sliding experiments in-situ in a scanning electron microscope (SEM). Through modifications to the SEM, these experiments could be run with a thin film of hydrocarbon oil applied to the sliding surface. Studies have been performed using AISI 4340 steel, both annealed and through hardened, for the pin and cylinder in combinations of soft (annealed)-versus-soft, hard-versus-soft and hard-versus-hard.

All three material combinations show a progressive smoothing in the wear track as the number of sliding passes increases, plus agglomeration of wear debris interspersed with oil around the contact. Both of these effects lead to failure of the contacts due to insufficient lubrication. The combinations involving annealed steel fail catastrophically by an apparent third body abrasive mechanism while the failure of the hard versus hard combination involves intermittent plowing, resulting in more localized damage.

INTRODUCTION

Many advances have been made in the understanding of boundary lubricated wear processes since the original definition of this lubrication regime was proposed by Hardy (*1*), (*2*). But, as many reviews of boundary lubrication point out (*3*), (*4*), (*5*), there is still much to be learned about the operative wear mechanisms and the variables that influence whether a lubricated contact will slide successfully. Among the less understood factors that influence the sliding behavior of boundary lubricated contacts are the surface topography of the sliding components and the role of the wear debris that is generated by the sliding action.

One approach to gaining further information about wear mechanisms is to perform sliding experiments in-situ in a scanning electron microscope (SEM), thus observing deformation and wear processes in real time. A number of in-situ SEM wear studies have been performed (*6*)–(*24*). These were all basically unlubricated experiments that involved relatively gross deformations, which were observable over a short period of time. Many of these studies (*6*)–(*18*) involved a hard (e.g. diamond or tungsten carbide) slider on a metal, resulting in abrasion-dominated wear processes. Several (*19*)–(*24*) involved unlubricated metal sliding on metal, placing additional emphasis on the role of adhesion in the wear process.

Recently, a simple modification to a scanning electron microscope has allowed in-situ sliding experiments to be performed with a thin film of hydrocarbon oil lubricating the surfaces (*25*)–(*27*). These experiments have been aimed at investigating the operative wear mechanisms for steel sliding on steel with a simple lubricant that contains no surface active additives. The results to date, using a relatively soft steel, have supported the conclusion that surface finishing grooves and scratches act as essential lubricant reservoirs for an otherwise marginally lubricated contact. Wear debris agglomerations have also been hypothesized (*26*), (*27*) to have a detrimental effect as the capillarity of the small voids between agglomerated wear particles acts to trap lubricant and thus, draw it away from the sliding contact.

This paper describes further work with AISI 4340 steel sliding against itself in lubricated long-term experiments that were continuously observed during run-in, through normal sliding and in the process of failure. Failure was defined as the point at which macroscopic surface damage was observed. The differences in wear processes before and during failure are discussed for hardened and relatively soft versions of this steel.

EXPERIMENTAL APPARATUS AND PROCEDURE

A small pin-on-cylinder wear test apparatus, which has been described previously (*25*), (*26*), was used to run the multipass sliding tests. The wear tester was designed as a self-contained unit that could be mounted inside the scanning electron microscope for running in-situ wear experi-

*Current Address:
The Timken Company, Timken Research, Canton, Ohio 44706-2798

Presented as a Society of Tribologists and Lubrication Engineers paper at the ASME/STLE Tribology Conference in Baltimore, Maryland, October 16–19, 1988
Final manuscript approved July 22, 1988

ments. The wear test apparatus could also be mounted in an auxiliary motorized base and run outside of the SEM. The practical benefit of this is that segments of the sliding tests could be run outside of the SEM at increased sliding speed, allowing each complete wear test to be finished in a reasonable amount of time.

A schematic diagram of the wear tester is shown in Fig. 1. Small ball bearings lubricated with a small amount of vacuum oil support each end of the 31.8 mm-diameter rotating cylinder. A hinge-mounted, strain-gaged beam with flexures for both load and friction measurement loads the pin against the cylinder by means of an adjustable spring. The spring, which is not shown in Fig. 1, applies tension between points A and B. The pin is a 3.175 mm diameter rod with a conical tip (40 degree semi-apex angle). The end of the conical tip is machined and polished leaving a flat contact area that ranged from .16mm (0.0065 in) to 0.23 mm (0.009 in) in diameter in these tests. The test apparatus has adjustments for alignment of the pin tip on the cylinder.

The scanning electron microscope used incorporates a differential pumping modification (*25*) that allows a significant pressure differential to be maintained between the column and chamber of the SEM. By holding the chamber at a higher than normal operating pressure [between 27 Pa (0.2 Torr) and 65 Pa (0.5 Torr) in these tests], liquid-lubricated surfaces can be imaged with good resolution without allowing any significant contamination of the SEM column.

A low-alloy steel (AISI 4340: 0.40C, 1.80Ni, 0.80Cr, 0.25Mo) was used for both the pin and the cylinder in these tests. Tests were run with hardened steel (hardness: Rc 55) sliding against hardened steel, annealed steel (hardness: Rc 22) sliding against annealed steel and with a hardened pin on an annealed cylinder. The pin tips had a smooth polished surface while the surface of the cylinders was finished with a pattern of grooves (generated with abrasive paper). The technique used to generate a consistent pattern of grooves on the cylinder surfaces was previously described (*25*).

TEST PROCEDURE

Each of the sliding tests was started with the tester mounted inside the scanning electron microscope. After a few cylinder revolutions, the tester was then removed from the SEM and run at higher sliding speed outside of the SEM. Periodically, the wear test was interrupted for additional in-situ SEM viewing as well as other measurements. Because of the self-contained nature of the test apparatus, none of these interruptions to move the test into or out of the SEM required any disassembly or realignment of the test components.

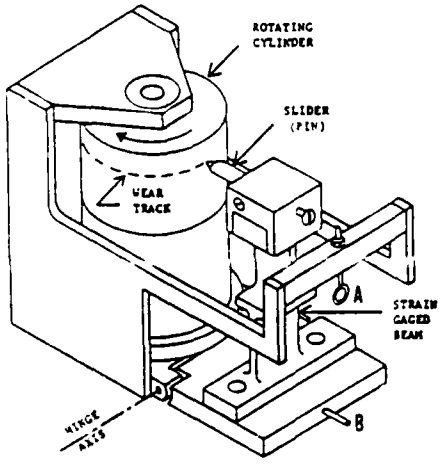

Fig. 1—Schematic Diagram of Pin-on-Cylinder Wear Tester. A spring in tension between points A and B applies load to the contact.

In all cases, the cylinder was lubricated once before each wear test by rubbing a thin film of molecularly distilled hydrocarbon oil (intended for vacuum applications) onto the sliding surface. This lubricant film, which was determined to be well under 1 μm in average thickness, was not replenished during the tests. The oil did not contain any surface active additives other than those which may have been formed as a result of oxidation or reaction of the oil during the tests.

Table 1 summarizes the experimental conditions for the tests that will be discussed in this paper. Additional wear tests were run for the hard-versus-hard and annealed-versus-annealed combinations, which will not be described in detail. The results of these additional tests support the qualitative conclusions of this work.

RESULTS-COEFFICIENT OF FRICTION

Figure 2 shows plots of coefficient of friction versus time for the three wear tests. The two solid lines plotted on Fig. 2 (a) and (b) show the upper and lower bounds of the friction values measured during the segments of each test that were run outside of the SEM. In the hard-versus-annealed test (Fig. 2 (c)), a few isolated areas on the cylinder surface had a coefficient of friction which was much higher than the range observed for the rest of the wear track. The shaded area on Fig. 2 (c) shows the range of coefficient of friction values measured in these isolated areas, while the two lines bounding the non-shaded area show the range of friction observed for the rest of the wear track. Figs. 2 (a)–(c) also show the range of coefficient of friction measured during the periodic in-situ, SEM segments of the tests by the two symbols connected by a vertical bar.

The friction data in Fig. 2 show the same basic pattern for all three wear tests. There is an initial period of smooth sliding where the friction is relatively low and steady, followed by rougher sliding and an increase in coefficient of friction. In all cases, this increase in friction at the end of the wear test occurred before and during failure of the surfaces. The observations made during these three wear tests and the condition of the failed surfaces will be described in the following sections.

RESULTS—HARDENED STEEL PIN VERSUS HARDENED STEEL CYLINDER

In SEM Observation of the Sliding Contact

Figure 3 shows a series of photomicrographs documenting the appearance of the contact throughout the wear test. The large, center photomicrograph shows the pin-on-cylinder contact during the first revolution of the test cylinder. A

TABLE 1—SUMMARY OF TEST CONDITIONS

HARDNESS (Rc)		LOAD	P/A STRESS	SLIDING SPEED (mm/s)		TEST DURATION
PIN	CYLINDER	[N (lb.)]	[MPa (psi)]	IN SEM	OUTSIDE SEM	[REVOLUTIONS]
55	55	5.29 (1.19)	183 (26 900)	0.014	0.834	7210
22	22	4.76 (1.07)	115 (16 800)	0.014	0.111	2070
55	22	4.80 (1.08)	222 (32 500)	0.014	1.66	206

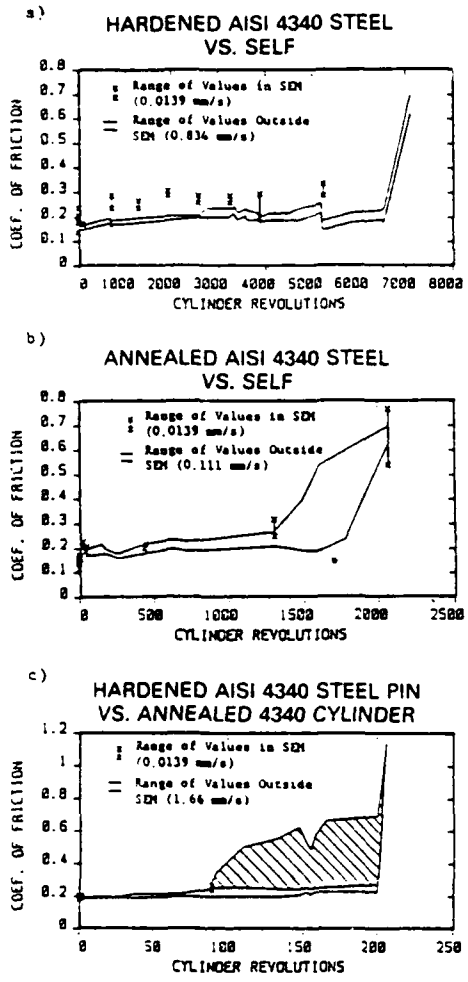

Fig. 2—Coefficient of Friction versus Time
(a) Hardened AISI 4340 steel pin versus hardened cylinder
(b) Annealed AISI 4340 steel pin versus annealed cylinder
(c) Hardened AISI 4340 steel pin versus annealed cylinder

small meniscus of oil, which appears black in the SEM, can be seen surrounding the contact. This meniscus built up during the early portions of all of the sliding tests and is supplied with oil by the initial film which is rubbed into the grooves and scratches on the cylinder surface.

The small photomicrograph in the upper left corner shows a view identical to the large center photo. The entire progression of wear can then be followed clockwise from the upper left corner. Note that the small photomicrographs are not all at the same magnification. For simplicity, micron bars have not been included with these photomicrographs.

At 700 revolutions, the meniscus is in the process of being replaced by a buildup of wear debris mixed with oil (third photomicrograph, top row). A similar appearance is seen in the increased amount of buildup at 1923 revolutions. Several areas of this buildup have the appearance of single, large flakes of debris. The photomicrograph of the leading edge of the pin taken at 3884 revolutions shows sheet-like forms plus long arms of debris extending forward from the contact. At this point in the sliding test (3884 revolutions), some of the leading edge buildup was carefully scraped from the pin with a fine copper wire and diluted with a clean mixture of solvent and mineral oil. A Ferrograph was then used to remove the wear particles from the mixture. All of the particles found were flat platelets of translucent reddish-brown oxide, identical in appearance to those identified as Fe_2O_3 in a wear debris reference atlas (*28*). While a few large oxide platelets were found on the slide (as big as 50 μm across), the vast majority appeared to be evenly distributed from about 10 μm down through the resolution limit of the microscope (well below 1 μm). This indicates that most of the complex debris shapes seen in Fig. 3 are not individual particles, but are agglomerates of these fine platelets, which are held together by the oil filling the spaces between them.

Figure 3 also shows that walls of debris slowly build up at the edges of the sliding track. At 700 revolutions a band

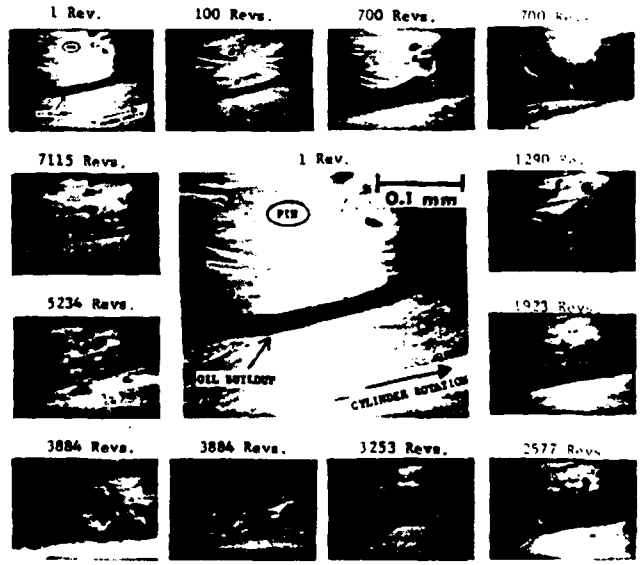

Fig. 3—SEM Photomicrographs of Hardened AISI 4340 Steel Pin Sliding on Cylinder of Same Material. Center photo shows enlargement of photo in upper left corner. Progression of wear clockwise from upper left corner.

of oil is visible at the edge of the track, which, with continued sliding, becomes more and more laden with wear debris. At the point on the cylinder where the photomicrograph corresponding to 2577 revolutions was taken (seventh photo on Fig. 3), this built up band is especially pronounced. The photomicrograph at 3253 revolutions shows a different location around the circumference of the cylinder where the bands of debris were somewhat less built up.

A few words of explanation are necessary for the last photomicrograph (7115 revolutions) in Fig. 3. At this point, the friction was extremely high which was usually indicative of surface damage due to failure of the contact in these tests. A large buildup of debris was observed optically. However, while mounting the tester in the SEM for video taping and photomicrographs, the cylinder was accidentally turned backwards for a very short distance, which dislodged most of the debris from the front of the pin. For this reason, the last photomicrograph on Fig. 3 (7115 revolutions) shows a reduced amount of debris buildup.

Wear Track Inspection

A series of SEM photomicrographs of the cylinder wear track, relocated on the same spot each time, is shown in Fig. 4. The column of photomicrographs on the left side of the Fig. 4 shows a low magnification view of the wear track. An enlarged slice across the wear track is shown to the right of each of these low magnification images. Because of space limitations, additional photomicrographs that showed no significant changes in the sliding surface have not been included. Because the wear track could not be identified early in the test, the photomicrographs for 2 and 100 revolutions have also been omitted.

Figure 4 shows a gradual smoothing of the cylinder surface. Slight grooving in the direction of sliding is also visible. Close examination of the wear track revealed that the smoothing that was occurring was basically the result of attrition, i.e. removal of metal rather than redistribution through deformation. Two enlarged photomicrographs of the relocation area taken at 700 and 2577 revolutions [Fig. 5 (a) and (b)] show that while some extrusion of metal is filling in a large scratch, most of the grooves and scratches are being smoothed out by abrasion of the surface (i.e. the surface is being worn down to the bottom of the grooves). The photomicrographs show that most of the original grooves had disappeared by the time the wear test had run for 3253 revolutions. At 5234 revolutions, the surface was still quite smooth, but a continued abrasive action was causing more new grooves to form along the wear track also.

The bottom photomicrographs on Fig. 4 show the appearance of the wear track after the sudden jump in friction at the end of the test. A central band of damage is visible which is the result of localized plowing. This damaged band was not continuous. Figure 6 shows an isolated plowing contact some distance upstream from the relocation area where the damage is restricted to a small area. The region surrounding this small gouge appears to be undamaged. Continued sliding for 95 more cylinder revolutions resulted in enlargement of some of these gouges as well as the formation of new damaged areas.

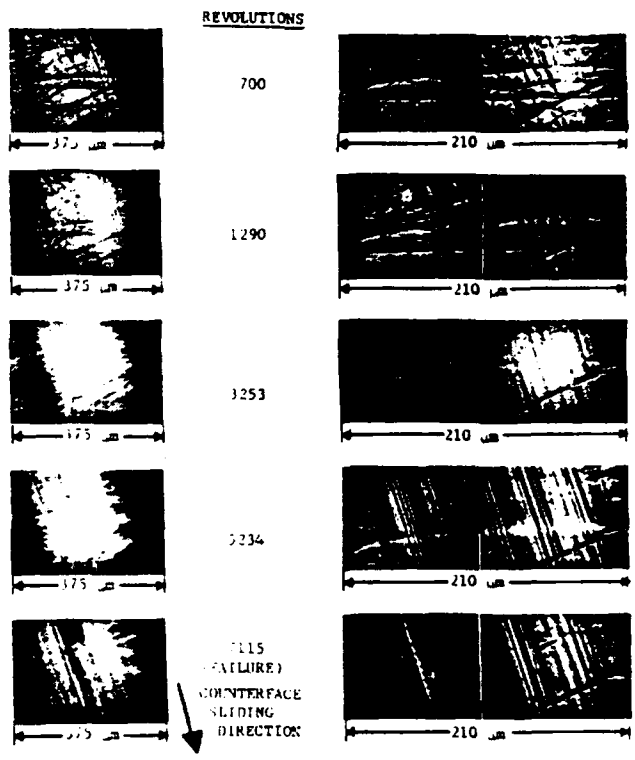

Fig. 4—SEM Photomicrographs of Wear Track on Hardened AISI 4340 Steel Cylinder, After Sliding Against Hardened AISI 4340 Steel Pin for Number of Revolutions Shown. Left side—low magnification. Right side—enlarged view of left side photomicrograph.

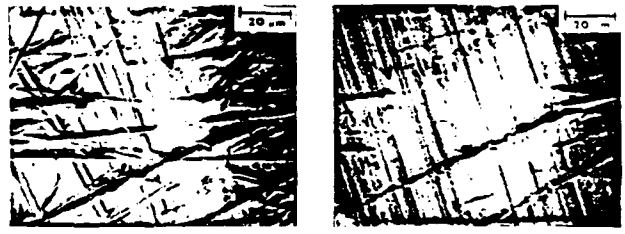

Fig. 5—SEM Photomicrographs of Wear Track for Hardened AISI 4340 Steel versus Self. (a) 700 revolutions; (b) 2577 revolutions. Arrow shows counterface sliding direction. (Magnification 1000x).

Surface Topography Measurements

Figure 7 shows a series of surface profiles of the test cylinder, taken circumferentially (i.e. along the wear track). The measured average roughness (R_a, 0.25 mm cut-off) and skewness (R_{sk}) are also shown adjacent to the profiles. These profiles show the gradual smoothing of the wear track from 2 through 3884 cylinder revolutions and the failed surface at 7210 revolutions. Although the average roughness of the last profile is among the lowest measured throughout the test at this location, the predominance of peaks in the profile, due to isolated areas of raised material, indicates that some surface damage has occurred.

RESULTS—ANNEALED STEEL VERSUS ANNEALED STEEL

The results of this wear test have been described in detail

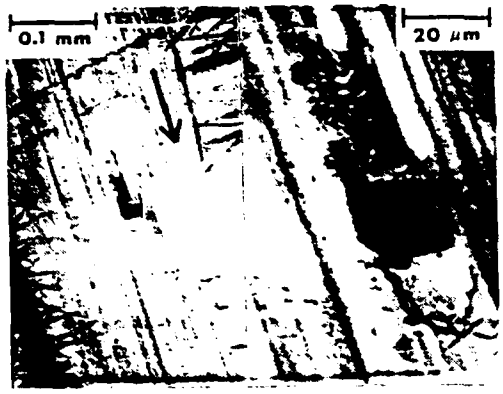

Fig. 6—SEM Photomicrographs (Left Side—200x; Right Side—1000x Enlargement of Boxed Area) of Wear Track on Hardened AISI 4340 Steel Cylinder After 7115 Revolutions. Arrow shows sliding direction of hardened steel counterface.

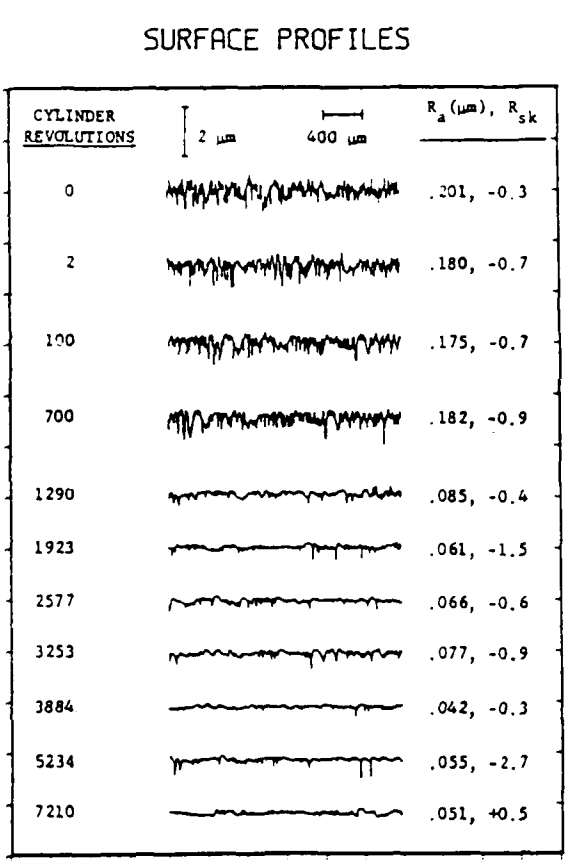

Fig. 7—Surface Profiles, Average Roughness (R_a) and Skewness (R_{sk}) of Cylinder Wear Track at Various Stages During Long Term Wear Test of Hardened AISI 4340 Steel Pin versus Annealed AISI 4340 Steel Cylinder. Bottom profile shows damaged area on surface.

in a previous paper (*26*) and are included here primarily as a basis for comparison with other tests. The continued sliding passes of the pin caused a plastic smearing of metal to slowly fill in the original surface finishing grooves on the cylinder. It was speculated that the smoothing resulted in a loss of lubricant retention capability in the surface, which eventually resulted in failure due to lack of lubrication at approximately 2060 revolutions. The failed surface, described in detail in (*26*), showed excessive cutting and plowing, including the formation of a cutting chip at the leading edge of the contact. The sequence of events in this test and the wear process during failure were very similar to the test of a hardened pin versus annealed cylinder which will be described in more detail in the next paragraphs.

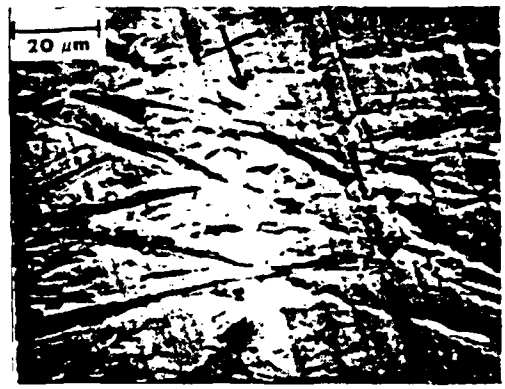

Fig. 8—SEM Photomicrograph of Wear Track on Annealed AISI 4340 Cylinder After 90 Revolutions Against Hardened Pin. Arrow shows counterface sliding direction. (Magnification—1000x).

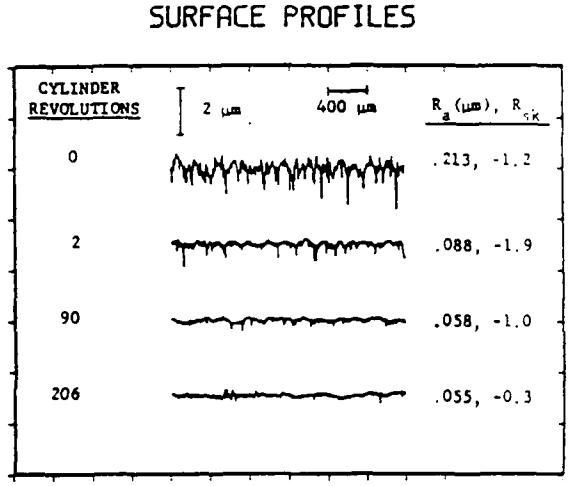

Fig. 9—Surface Profiles, Average Roughness (R_a) and Skewness (R_{sk}) of Cylinder Wear Track at Various Stages During Long Term Wear Test of Hardened AISI 4340 Steel Pin versus Annealed AISI 4340 Steel Cylinder.

RESULTS—HARDENED STEEL PIN VERSUS ANNEALED STEEL CYLINDER

The friction versus time plot for this test, shown in Fig. 2, once again indicates that the friction became higher and more erratic as the sliding test progressed. The surface of the cylinder was becoming smoother as shown in the photomicrograph in Fig. 8, taken at 90 revolutions. Plastic flow of metal can be seen which is contributing to the smoothing of the wear track. The surface profiles in Fig. 9 also show the rapid smoothing of the surface during the first 90 passes of the hardened steel pin.

This test suddenly failed at 206 cylinder revolutions. Figure 10 shows the observed result: the formation of a

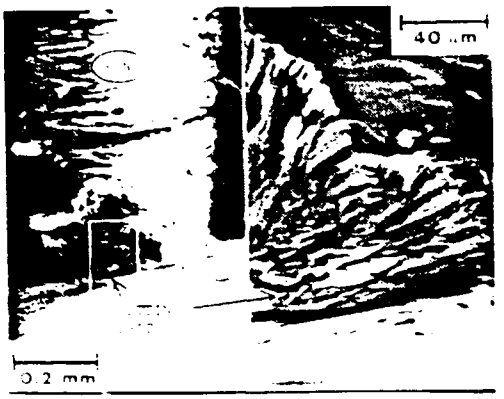

Fig. 10—SEM Photomicrographs (Left Side—100x; Right Side—500x Enlargement of Boxed Area) of Cutting Chip Formation at Leading Edge of Pin-on-Cylinder Contact. Materials: Hardened AISI 4340 steel pin versus annealed AISI 4340 steel cylinder.

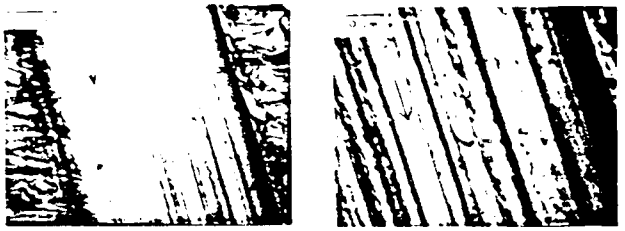

Fig. 11—SEM Photomicrographs of Failed, Annealed AISI 4340 Steel Cylinder After 206 Passes of Hardened Pin. Arrows show counterface sliding direction. [Magnifications: (a) = 400x, (b) = 1000x].

Fig. 12—SEM Photomicrograph of Tip of Hardened AISI 4340 Steel Pin After 206 Cylinder Revolutions. Arrow shows sliding direction of annealed steel counterface. (Magnification = 400x).

cutting chip. The appearance of the failed wear track is shown in Fig. 11, and a corresponding photomicrograph of the tip of the hardened steel slider is shown in Fig. 12. As previously observed with an annealed steel slider (26), furrows are cut along the wear track by individual high features and adhered particles of wear debris on the pin tip. The continuous chip is the manifestation of this cutting action when the penetration occurs at the leading edge of the contact.

METALLURGICAL EXAMINATION OF WEAR TRACKS

After the wear tests, a portion of the failed wear track on the circumference of the cylinder for the annealed vs. annealed and the hard vs. hard test was polished by metallographic techniques until the wear track in a small part of this segment was completely removed. Thus, when each cylinder was rotated through a small arc for inspection, the portion of the track between the polished area and the undisturbed area showed the appearance of the wear track at various depths. This polished area was then lightly etched, using a 2 percent picral solution, and the specimen was examined in the scanning electron microscope.

Although both the hardened and the annealed AISI 4340 steel cylinders appear to undergo deformation in the wear track, the type of deformation is distinctly different. Figure 13 shows electron micrographs of the condition of the wear track in the hardened steel surface. The overall microstructure is fine grained, tempered martensite. The grooves within the wear track are surrounded by voids indicating grain boundary failure. There is very little deformation within the grains themselves. Essentially, the shape of a crystal and its neighboring crystals coincides except for the void area around the grains. Some of the smaller grains have been removed and the remaining void geometry is similar to that of the typical crystalline structure. In the area outside of the wear track there is no space between the grains indicating that the metallographic polishing did not cause the grain boundary condition in the wear track. It appears that during the sliding process the grain boundaries are weakening and smaller grains are being removed, possibly as grains rub together due to elastic deformation under load.

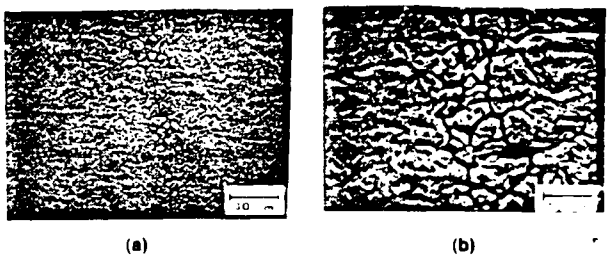

Fig. 13—Typical Appearance of the Wear Track on the Hardened AISI 4340 Steel Surface Showing Breakdown at the Grain Boundaries. Specimen surface has been metallographically polished and etched. [Magnifications: (a) = 650x, (b) = 2400x].

The track on the softer steel shows gross deformation throughout (Fig. 14). It is difficult to identify any individual grains in Fig. 14. Areas outside of the wear track which had been metallographically polished show no deformation and no metal smearing. Hence, most of the wear track has been plastically deformed, with metal smearing as the predominant deformation mechanism.

DISCUSSION

These experiments were run under very severe sliding conditions. The high contact stresses and low sliding speeds precluded the generation of fluid film effects so that the lubricant must have protected the surfaces on a molecular level. Thus, supply of oil to and retention of oil within the contact become essential factors. The in-situ SEM observations made in these studies have shown that the grooves

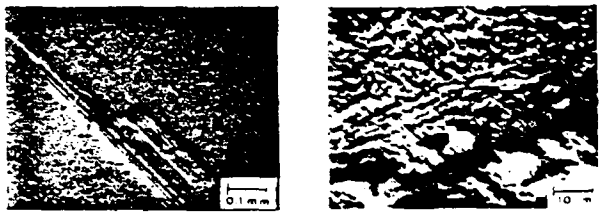

(a) (b)

Fig. 14—Typical Appearance of the Wear Track on the Annealed AISI 4340 Steel Surface Showing Gross Deformations. Specimen surface has been metallographically polished and etched. [Magnifications: (a) = 170x, (b) = 1700x].

on the surface of the test cylinder act as reservoirs to hold oil. Figure 10 in Ref. (25) shows this quite clearly. Since there is no replenishment of lubricant in these tests, any loss of lubricant retaining grooves may be detrimental to the sliding behavior. The severe sliding conditions and poor lubrication should act to accelerate effects that could also occur in a normal, well-lubricated contact.

A possible sequence of events in these experiments, based on the observations made, is that the run-in phase involves a progressive change in surface topography from a surface consisting of relatively random hills and valleys to a surface consisting of smooth, flat lands interrupted by scratches and grooves. This run-in is accompanied by a build-up of fine wear debris interspersed with oil around the pin-on-cylinder contact. As sliding progresses, the processes initiated during the run-in phase continue and result in a loss of lubricant reaching the contact, because the oil-retaining reservoirs are being eliminated and the remaining oil is being tied up in debris/oil agglomerates. These clumps of debris/oil build up at the leading edge of the pin and eventually are deposited on the cylinder alongside the wear track, either as separate clumps or as continuous walls on either side of the track (see Fig. 3). Other investigators have suggested that debris collects in the scratches and grooves within a wear track (11), (29), but this has not been observed in the current studies.

The loss of the protective lubricant barrier between the metal surfaces may result in localized adhesion of the surfaces and the formation of relatively large wear particles. The wear then perpetuates itself to catastrophic failure because trapped wear particles cause an acceleration of the damage. The failure involves adhesion plus significant plowing and penetration, i.e. abrasive processes. Bates et al (9) have coined the term "penetrative wear" for processes such as this in which both adhesion and abrasion play a role in the wear process.

The effect of steel hardness on abrasion resistance has been studied for a number of years. Often quoted is the fundamental work of Kruschov (30) and Rabinowicz (31), which showed that for any given metal, the abrasive wear resistance improves as the metal hardness is increased. Kragelski (32) has also discussed this in detail. Murray et al (33) attempted to better quantify the relationship between hardness, attack angle (related to penetration) and abrasive wear resistance, and showed that a transition from plowing to cutting occurs if the metal hardness is reduced. Unlubricated in-situ SEM scratch tests, by Kayaba et al (14) and Hokkirigawa and Li (15), visually confirmed the hardness effect as well as adding valuable quantitative information on the relationship between groove volume and the actual volume of material removed by wear. The present lubricated studies show the same effects during failure of a marginally lubricated contact.

The loss of lubricant retaining grooves, which is a key element of this discussion, appears to be the result of two processes in the steels of different hardnesses. For the annealed steel cylinder with an annealed steel pin, the grooves are slowly covered over by plastically smeared metal. For the annealed steel cylinder with a hardened steel pin the process is essentially the same, but the progression to failure occurs much more quickly. For the hardened steel combination, plastic flow is minimized and the higher features on the cylinder are worn down by a process that apparently involves abrasion. Thus, the surface wears down to the bottom of the grooves.

The differing character between the annealed steel and the hardened steel is predicted by elastic/plastic contact parameters, such as the plasticity index (Ψ). The plasticity index, first introduced by Greenwood and Williamson (34) and modified by Hirst and Hollander (35) predicts the degree of plastic deformation that will occur when rough surfaces are loaded in contact. It is given by

$$\Psi = 0.6 \frac{E' R_q}{H \beta^*}$$

where

E' = reduced elastic modulus for the contacting materials, i.e. $1/E' = 1/E_1 + 1/E_2$
H = penetration hardness of softer material
R_q = RMS average roughness
β^* = correlation length (a surface "wavelength" parameter)

The values of Ψ, R_a, R_q and β^* for the series of surface profiles in Fig. 7 and 9, plus values previously calculated (26) for the annealed versus annealed combination are shown in Table 2.

A plasticity index value greater than the threshold value of $\Psi = 1$ predicts a significant number of plastic asperity contacts. Thus, significant plastic flow upon contact is predicted for the first three profile measurements for the annealed steel couple and the first measurement for the hard-on-annealed combination. Table 2 shows that no plastic flow is predicted for the hard-on-hard combination, thus agreeing with the behavior that was actually observed in these tests.

CONCLUSIONS

By performing steel-on-steel sliding experiments in-situ in a scanning electron microscope with a thin film of hydrocarbon oil lubricating the sliding surfaces, the following observations were made:

1. After repeated sliding passes, the surfaces fail due to

TABLE 2—SURFACE TOPOGRAPHY PARAMETERS

CYLINDER REVOLUTIONS	R_a (μm)	R_q (μm)	β* (μm)	Ψ
HARDENED STEEL PIN SLIDING ON HARDENED STEEL CYLINDER				
0	0.201	0.249	9.12	0.628
2	0.180	0.229	7.48	0.703
100	0.175	0.216	10.70	0.465
700	0.182	0.228	11.18	0.468
1290	0.085	0.107	15.95	0.154
1923	0.061	0.087	10.60	0.188
2577	0.066	0.089	13.82	0.148
3253	0.077	0.067	19..11	0.081
3884	0.042	0.060	18.92	0.073
5243	0.055	0.069	25.16	0.063
7210	0.051	0.036	73.55	0.011
ANNEALED STEEL PIN SLIDING ON ANNEALED STEEL CYLINDER				
CYLINDER REVOLUTIONS	R_a (μm)	R_q (μm)	β* (μm)	Ψ
0	0.329	0.425	8.87	1 33
2	0.296	0.365	5.39	1 89
36	0.259	0.334	7.37	1 27
150	0.091	0.163	12.00	0.38
443	0.069	0.131	11.17	0.33
618	0.059	0.084	14.07	0.17
1303	0.045	0.088	11.34	0.22
1783	0.039	0.049	23.42	0.06
2070	0.139	0.191	26.38	0.20
HARDENED STEEL PIN SLIDING ON ANNEALED STEEL CYLINDER				
CYLINDER REVOLUTIONS	R_a (μm)	R_q (μm)	β* (μm)	Ψ
0	0.231	0.287	9.11	1.735
2	0.088	0.126	10.09	0.687
90	0.058	0.074	31.89	0.128
206	0.055	0.072	28.61	0.139

lack of lubrication. It is believed that oil is prevented from reaching the contact because smoothing of the surfaces results in a loss of essential lubricant reservoirs. Additionally, oil is lost from the contact as it is tied up in wear debris/oil agglomerates.

2. The surface smoothing that takes place involves plastic flow of metal to fill in the original grooves and scratches on the softer steel surface, while the harder surface wears down to the bottom of the grooves.
3. The crystal structure of the hardened steel showed little plastic deformation in the wear track but the individual grains were surrounded by void. The track in the annealed steel showed gross deformation and individual crystals could not be identified.
4. Cutting by trapped wear debris is the predominant mechanism of wear during failure of the softer steel. The harder steel wears by a plowing mechanism during failure.

ACKNOWLEDGMENTS

Financial support for this work was provided under U.S. Army Research Office Contract DAAL-03-86-K-0076. Also acknowledged is the surface topography equipment provided by the National Science Foundation under Grant MSM-8505954.

REFERENCES

(1) Hardy, Sir Wm. and Doubleday, I., "Boundary Lubrication—The Paraffin Series," *Proc. Roy. Soc. A.*, **102**, pp 550–574 (1922).
(2) Hardy, Sir Wm., "Problems of the Boundary State," *Phil. Trans. Roy Soc. A.*, **230**, pp 1–37 (1931).
(3) Campbell, W. E., "Boundary Lubrication," in *Boundary Lubrication. An Appraisal of World Literature*, Ling, F. F., Klaus, E. E. and Fein, R. S. eds., ASME, New York, NY, pp 87–117 (1969).
(4) Godfrey, D., "Boundary Lubrication," in *Interdisciplinary Approach to Friction and Wear*, Ku, P. M. ed., **NASA SP-181**, pp 335–384 (1968).
(5) Barwell, F. T., "Wear of Machine Elements," in *Fundamentals of Tribology*, Suh, N. P. and Saka, N., eds., MIT Press, Cambridge, MA, pp 401–442 (1980).
(6) Gane, N. and Bowden, F. P., "Microdeformation of Solids," *J. of Applied Physics*, **39**, 3, pp 1432–1435 (1968).
(7) Skinner, J., Gane, N. and Tabor, D., "Micro-friction of Graphite," *Nature Physical Science*, **232**, pp 195–196 (1971).
(8) Gane, N. and Skinner, J., "The Friction and Scratch Deformation of Metals on a Micro Scale," *Wear*, **24**, pp 207–217 (1973).
(9) Bates, T. R., Jr., Ludema, K. C. and Brainard, W. A., "A Rheological Mechanism of Penetrative Wear," *Wear*, **30**, pp 365–375 (1974).

(10) Brainard, W. A. and Buckley, D. H., "Dynamic SEM Wear Studies of Tungsten Carbide Cermets," *ASLE Trans.*, **19**, 4, pp 309–318 (1976).
(11) Glaeser, W. A., "Wear Experiments in the Scanning Electron Microscope," *Wear*, **73**, pp 371–386 (1981).
(12) Kavaba, T., Kato, K. and Nagasawa, Y., "Abrasive Wear in Stick-Slip Motion," *Proc. Int. Conf. on Wear of Materials*, San Francisco, California, Mar. 30–Apr. 1, 1981; ASME, New York, NY, pp 439–446 (1981).
(13) Kato, K. and Hokkirigawa, K., "Abrasive Wear Diagram," EUROTRIB 85—*Proc. 4th European Tribology Congress*, Elsevier Science Pub. Co., New York, NY, **Session 5.3** (1985).
(14) Kavaba, T., Hokkirigawa, K. and Kato, K., "Analysis of the Abrasive Wear Mechanism by Successive Observations of Wear Processes in a Scanning Electron Microscope," *Wear*, **110**, pp 419–430 (1986).
(15) Hokkirigawa, K. and Li, Z. Z., "The Effect of Hardness on the Transition of Abrasive Wear Mechanism of Steels," *Proc. Int. Conf. on Wear of Materials*, Houston, TX, Apr. 5–9, 1987; ASME, New York, NY, pp 585–593 (1987).
(16) Ahman, L. and Oberg, A., "Mechanisms of Micro-Abrasion—In-Situ Studies in SEM," *Proc. Int. Conf. on Wear of Materials*, Reston, VA, Apr. 11–14, 1983, ASME, New York, NY, pp 112–120 (1983).
(17) Prasad, S. V. and Kosel, T. H., "In-Situ SEM Scratch Tests on White Cast Irons With Rounded Quartz Abrasive," *Proc. Int. Conf. on Wear of Materials*, Reston, VA, Apr. 11–14, 1983, ASME, New York, NY, pp 121–129 (1983).
(18) Kato, K., Hokkirigawa, K., Kavaba, T. and Endo, Y., "Three Dimensional Shape Effect on Abrasive Wear," *Trans. ASME—Journal of Tribology*, **108**, pp 346–351 (1986).
(19) Skinner, J. and Cane, N., "Sliding Friction Under a Negative Load," *J. Phys. D: Appl. Phys.*, **5**, pp 2087–2094 (1972).
(20) Brainard, W. A. and Buckley, D. H., "Dynamic-Scanning-Electron-Microscope Study of Friction and Wear," NASA TN D-7700 (1974).
(21) Tsuya, Y., Saito, K., Takagi, R. and Akaoka, J., "In-Situ Observation of Wear Process in a Scanning Electron Microscope," *Proc. Int. Conf. on Wear of Materials*, Dearborn, Michigan, Apr. 16–18, 1979, ASME, New York, NY, pp 57–71 (1979).
(22) Kavaba, T. and Kato, K., "The Analysis of Adhesive Wear Mechanism by Successive Observations of the Wear Process in SEM," *Proc. Int. Conf. on Wear of Materials*, Dearborn, Michigan, Apr. 16–18, 1979, ASME, New York, NY, pp 45–56 (1979).
(23) Calabrese, S. J., Ling, F. F. and Murray, S. F., "Dynamic Wear Tests in the SEM," *ASLE Trans.*, **26**, 4, pp 455–465 (1983).
(24) Lim, S. C. and Brunton, J. H., "A Dynamic Wear Rig for the Scanning Electron Microscope," *Wear*, **101**, pp 81–91 (1985).
(25) Holzhauer, W. and Calabrese, S. J., "Modification of SEM for In-Situ, Liquid-Lubricated Sliding Studies," *ASLE Trans.*, **30**, 3, pp 302–309 (1987).
(26) Holzhauer, W. and Ling, F. F., "In-Situ SEM Study of Boundary Lubricated Contacts," *TRIB Trans.* **31**, 3, pp 360–369 (1988).
(27) Holzhauer, W., "In-Situ SEM Study of Boundary Lubricated Sliding Contacts," **Ph.D. Thesis,** Rensselaer Polytechnic Institute, Troy, New York (December, 1987).
(28) Anderson, D. P., *Wear Particle Atlas*, SOHIO Predictive Maintenance Services, 30701 Carter Street, Solon, OH, 1982; *Naval Air Engineering Center*, Lakehurst, NJ, **Report NAEC-92-163** (1982).
(29) Komvopoulos, K., Discussion of Ref. (26) TRIB Trans. **31**, 3, pp 360–369 (1988).
(30) Kruschov, M. M., "Resistance of Metals to Wear By Abrasion, as Related to Hardness," *Proc. Conf. On Lubrication and Wear*, Institution of Mechanical Engineers, London, pp 655–659 (1957).
(31) Rabinowicz, E., *Friction and Wear of Materials*, John Wiley and Sons, Inc., New York, NY (1965).
(32) Kragelsku, I. V., *Friction and Wear*, Butterworth Inc., Washington, D.C. (1965).
(33) Murray, M. J., Mutton, P. J. and Watson, J. D., "Abrasive Wear Mechanisms of Steels," *Proc. Int. Conf. on Wear of Materials*, Dearborn, Michigan, Apr. 16–18, 1979; ASME, New York, NY, pp 257–265 (1979).
(34) Greenwood, J. A. and Williamson, J. B. P., "Contact of Nominally Flat Surfaces," *Proc. Roy. Soc. London A*, **295**, pp 300–319 (1966).
(35) Hirst, W. and Hollander, A. E., "Surface Finish and Damage in Sliding," *Proc. Roy. Soc. London A*, **337**, pp 379–394 (1974).